

Annealed proton-exchanged LiNbO₃ waveguides

M. L. Bortz and M. M. Fejer

Edward L. Ginzton Laboratory, Stanford University, Stanford, California 94305

Received April 12, 1991

We report characterization of annealed proton-exchanged waveguides in LiNbO₃. Effective-mode indices and fundamental-mode intensity profiles were measured for a variety of fabrication conditions. Index profile, depth, and surface refractive-index change were determined versus exchange depth and anneal time and are presented in a universal form. An empirical concentration-dependent diffusion model describing the annealing process is presented. The refractive-index dispersion in proton-exchanged and annealed proton-exchanged waveguides was determined for wavelengths between 0.4 and 1.1 μm .

The annealed proton-exchange (APE) process has emerged as an important technique for the fabrication of low-loss optical waveguides in LiNbO₃. Unannealed proton-exchanged (PE) waveguides have steplike refractive-index profiles and large extraordinary refractive-index changes ($\Delta n_e \approx 0.125$ at $0.633 \mu\text{m}$).¹⁻³ Postexchange annealing is necessary to produce stable, single-mode, low-loss waveguides that exhibit nonlinear optical properties comparable with those of bulk LiNbO₃ (Ref. 4) and good coupling to fibers.⁵ Although the PE process has been widely studied, quantitative models that predict the modal properties of APE waveguides from processing parameters are unavailable. In this Letter we present measurements of the effective-mode indices and fundamental-mode profiles for APE waveguides subjected to a variety of exchange and annealing conditions. We also present empirical models for the diffusion coefficient and dispersion that permit accurate calculation of the refractive-index profile for APE waveguides as a function of exchange depth and anneal time for wavelengths between 0.4 and 1.1 μm .

Planar PE waveguides were fabricated on *z*-cut LiNbO₃ with the use of pure benzoic acid at temperatures between 160 and 220°C. Exchange depths (d_e) were calculated by using the expression in Ref. 2 and ranged from 0.15 to 0.50 μm . All annealing was performed in air at 333°C for times (t_a) between 1.3 and 40 h. TM effective-mode indices were measured with the use of the standard prism coupling technique at a wavelength $\lambda = 0.458 \mu\text{m}$ to maximize the number of modes. Low powers were used to avoid potential photorefractive effects. A photodiode array was used to improve the precision of the effective-index measurements, and care was taken to measure the LiNbO₃ substrate refractive index. Reproducibility in the effective indices was ± 0.0001 .

Typical index profiles [$\Delta n(z)$] for three APE waveguides, derived by use of the IWKB technique,⁶ are shown in Fig. 1. Uncertainties in the surface refractive-index changes (Δn_a) vary with the number of modes and profile shape and range from a maximum of $\sim 10\%$ for waveguides with the highest sur-

face index to $< 5\%$ for highly annealed guides with many modes. The steplike profile evolves to an approximately exponential form as previously observed⁷ and, with continued annealing, to a Gaussian form. The $1/e$ depths (d_a) and surface-index changes of the APE waveguides, normalized to the depths and surface-index changes before annealing ($\Delta n_e = 0.184$ at $\lambda = 0.458 \mu\text{m}$), are plotted in Fig. 2 versus the square root of the normalized anneal time, defined as $\tau = t_a/d_e^2$. For short anneal times, the waveguide depths increase sublinearly with $\sqrt{\tau}$ but approach a linear regime for $\sqrt{\tau} > 8\sqrt{h}/\mu\text{m}$. In this latter regime this slope corresponds to a constant diffusion coefficient of $D_0 = 0.55 \mu\text{m}^2/\text{h}$. Calculation of the depth from a linear diffusion model with this D_0 yields the dashed curves shown in Fig. 2, which clearly disagree with the data for all τ and suggest that linear diffusion models^{8,9} are inadequate for describing the APE process.

Analysis of the APE process is complicated by both nonlinear diffusion and a refractive-index change that is reported to be highly nonlinear with proton concentration.¹⁰ This latter behavior manifests itself as a variation in the area under the IWKB index profile during annealing, and previous reports for *x*-cut substrates indicate area increases of $\sim 30\%$ for initial exchange depths of $\sim 2.5 \mu\text{m}$.⁷ Recent reports indicate a more linear dependence of the index on proton concentration,¹¹ for which smaller variations in the IWKB areas are predicted. For all the waveguides shown in Figs. 1 and 2, the area under the refractive-index profile normalized to the exchange depth was constant to within the experimental resolution of 5%, with the exception of the waveguide shown in Fig. 1(a) with $\Delta n_a = 0.14$. This waveguide had the highest surface-index change studied and an area increase of $\sim 20\%$. The nearly linear relationship between index change and concentration allows an identification of the refractive-index profiles with concentration profiles over the range of concentrations relevant to the analysis of the data presented here.

Although the universal curves presented in Fig. 2 are adequate for predicting d_e and Δn_a for planar waveguides, an analytical diffusion model for the

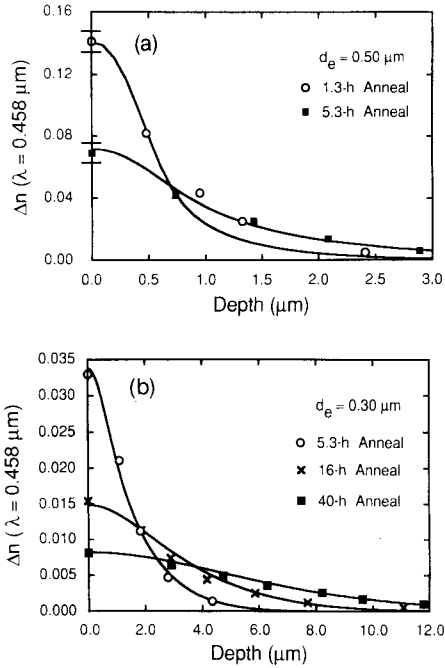


Fig. 1. IWKB refractive-index profiles for APE waveguides with (a) $d_e = 0.50 \mu\text{m}$, (b) $d_e = 0.30 \mu\text{m}$, and various anneal times. The curves are the results of the model described in the text. Note the systematic error in the model for the shortest anneal time.

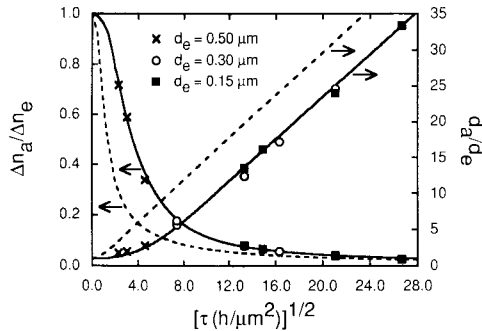


Fig. 2. Normalized index change and waveguide depth versus the square root of the normalized anneal time. The dashed line and curve are the predictions of linear diffusion theory with $D_0 = 0.55 \mu\text{m}^2/\text{h}$. The solid curves are the results of the nonlinear diffusion model described in the text.

transport of protons during the annealing process would be useful for modeling channel waveguides. A complete model of diffusion in a polyphase system such as $\text{H}_x\text{Li}_{1-x}\text{NbO}_3$ (Ref. 12) is extremely complicated, involving the solid solubilities and the concentration-dependent diffusion coefficients in each of the phases combined into a nonlinear moving-boundary diffusion problem. The analysis is further complicated by the possibility of interface kinetic limitations influencing the transport. Although it is not obvious from these considerations that a continuous-diffusion coefficient in a simple diffusion equation is adequate to describe the APE process, we found empirically that such a model, together with a linear relation between concentration and index of refraction given by $\Delta n(z) = 1.06\Delta n_e C(z)$, could quantitatively predict the ob-

served refractive-index profiles within the error of the IWKB analysis over a broad range of fabrication parameters. We took the step-profile² characteristic of PE as the initial condition and modeled the annealing process by numerically integrating the one-dimensional diffusion equation with a concentration-dependent diffusion coefficient of the form

$$D(C) = D_0[a + (1 - a)\exp(-bC)], \quad (1)$$

where C is the H^+ concentration normalized to its initial value after proton exchange, $D_0 = 0.55 \mu\text{m}^2/\text{h}$ is the asymptotic diffusion coefficient for low proton concentrations, and the free parameters a and b that best fit the model to the data take the values 0.1 and 12, respectively. Refractive-index profiles generated with the use of this model are shown in Fig. 1 as solid curves. Normalized quantities d_a/d_e and $\Delta n_a/\Delta n_e$ versus $\sqrt{\tau}$ over a wide range of exchange-anneal conditions are shown in Fig. 2 as solid curves and are in good agreement with the IWKB results. This model accurately reproduces all the experimental refractive-index profiles except for the waveguide that has the largest ($\Delta n_a = 0.14$) index change, shown in Fig. 1(a).

It is difficult to assign any microscopic significance to a diffusion coefficient used to describe transport in a two-phase mixture, corresponding to $0.12 \leq 0.55$ for $\text{H}_x\text{Li}_{1-x}\text{NbO}_3$.¹² It is best to view Eq. (1) as a purely empirical quantity that accurately predicts experimental observations, noting that its success suggests that, over the range of parameters investigated here, interface kinetic effects are not the rate-limiting step in the transport. The discrepancy between the predictions of the model and the observed refractive-index profile for the lowest value of τ indicates that the model is incomplete, but the agreement with the rest of the data indicates that this limitation is confined to high proton concentrations. In typical APE processes, a shallow exchange layer must be annealed to $d_a/d_e \approx 7$ to reduce the concentration to the α phase.¹¹ Because we are primarily interested in the final profile of the waveguide after annealing to low concentrations rather than the behavior during exchange (which is adequately described by an effective-diffusion coefficient controlling the depth of a step profile) or the transient regime at high concentrations during the first stages of annealing, the inaccuracy of the model

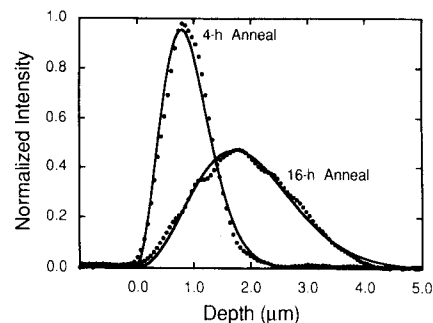


Fig. 3. Measured ($\lambda = 0.458 \mu\text{m}$) and calculated fundamental-mode intensity profiles for waveguides with $d_e = 0.15 \mu\text{m}$ and different anneal times.

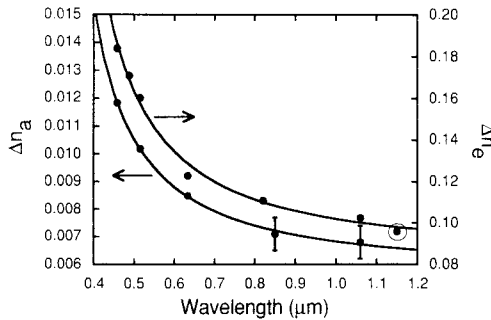


Fig. 4. Dispersion in PE and APE waveguides. The circled point, for an x -cut PE waveguide, is from Ref. 3.

at high concentrations is not a serious limitation. It is difficult to make meaningful comparisons between our model and previous interdiffusion models^{2,8} because the latter were developed to account for the step-profile characteristic of PE and are inconsistent with IWKB data for annealed waveguides.

The form assumed for the dependence of the refractive index on concentration clearly cannot apply for $C = 1$, indicating saturation of the index at high concentrations. The precise nature of the saturation is not relevant to the interpretation of our data, which are all (with the exception of the waveguide with $\Delta n_a = 0.14$) taken for surface concentrations sufficiently low that the area of the refractive-index profile is constant. The slope that we postulate is in reasonable agreement with the data of Ref. 11 up to $x = 0.6$. A further complication in interpreting the refractive-index data is the temperature-dependent H^+ outdiffusion, recently shown to be significant at anneal temperatures of 400°C.¹³ Further study is necessary to resolve this point.

Two further tests were performed to verify the accuracy of the model at $\lambda = 0.458 \mu\text{m}$. The observed effective-mode indices for a variety of few-mode APE waveguides were compared with modal dispersion curves¹⁴ calculated by using the index profiles determined by the model. The values for d_a and Δn_a obtained with the use of this analysis were in good agreement with the IWKB technique. Also, fundamental-mode intensity profiles were imaged and compared with numerical solutions of the scalar wave equation for index profiles derived by using Eq. (1). Mode shapes measured with the use of a CCD array and a multiple-stage imaging system are in good agreement with theoretical predictions, as shown in Fig. 3 for waveguides exchanged to $d_e = 0.15 \mu\text{m}$ and annealed for 4 and 16 h.

Knowledge of the dispersion in the surface refractive index is necessary to design waveguides at wavelengths other than $\lambda = 0.458 \mu\text{m}$. We measured the effective-mode indices at wavelengths between 0.4 and 1.1 μm for a PE and an APE waveguide. The PE waveguide was 2.5 μm deep, whereas the APE waveguide was exchanged to $d_e = 0.30 \mu\text{m}$ and annealed for 24 h. The surface-index change of the PE waveguide was determined by using modal dispersion curves generated by assuming a step profile. Depending on the number of guided modes at a particular wavelength, Δn_a of the

APE waveguide was found either by using IWKB analysis of the effective indices or by comparing the measured indices with the mode spectrum calculated with the use of the index profile shape derived by the model. For each waveguide the $1/e$ depth was found to be independent of wavelength. Dispersion data in Δn for the two waveguides, along with single-pole Sellmeier fits, are shown in Fig. 4.¹⁵ Error increases in the infrared owing to difficulties in measuring the substrate index. The ratio of the index changes for the two waveguides is nearly independent of wavelength, even though for the annealed guide $\Delta n_a < 0.01$ at 0.633 μm , indicating a dilute proton concentration. Thus to a good approximation the dispersion is constant during the annealing process. The dispersion data contained in Fig. 4 may be used to scale the refractive-index profiles determined by using Eq. (1) to other wavelengths.

Extension of this research to x -cut LiNbO_3 substrates to develop a two-dimensional description of the APE process is in progress.

The authors thank P. F. Bordui, E. J. Lim, W. M. Young, and M. M. Howerton for useful discussions and the Defense Advanced Research Projects Agency, the Joint Services Electronics Program, and Crystal Technology, Inc., for support.

References

1. J. L. Jackel, C. E. Rice, and J. J. Veselka, *Appl. Phys. Lett.* **41**, 607 (1982).
2. D. F. Clark, A. C. G. Nutt, K. K. Wong, P. J. R. Laybourn, and R. M. De La Rue, *J. Appl. Phys.* **54**, 6218 (1983).
3. K. K. Wong, A. C. G. Nutt, D. F. Clark, J. Winfield, P. J. R. Laybourn, and R. M. De La Rue, *IEE Proc. Pt. J* **133**, 113 (1986).
4. P. G. Suchoski, T. K. Findakly, and F. J. Leonberger, *Opt. Lett.* **13**, 1050 (1988).
5. J. J. Veselka and G. A. Bogert, *Electron. Lett.* **23**, 265 (1987).
6. J. M. White and P. F. Heidrich, *Appl. Opt.* **15**, 151 (1976).
7. K. K. Wong, *Proc. Soc. Photo-Opt. Instrum. Eng.* **993**, 13 (1988).
8. S. T. Vohra, A. R. Mickelson, and S. E. Asher, *J. Appl. Phys.* **66**, 5161 (1989).
9. W. Charczenko, M. Surette, and A. R. Mickelson, in *Digest of Conference on Integrated Photonics Research* (Optical Society of America, Washington, D.C., 1991), TUC3.
10. C. E. Rice, J. L. Jackel, and W. L. Brown, *J. Appl. Phys.* **57**, 4437 (1985).
11. M. M. Howerton, W. K. Burns, P. R. Skeath, and A. S. Greenblatt, *IEEE J. Quantum Electron.* **27**, 593 (1991).
12. C. E. Rice, *J. Solid State Chem.* **64**, 188 (1986).
13. Y. S. Son, H. J. Lee, and S. Y. Shin, *IEEE Photon. Technol. Lett.* **2**, 184 (1990).
14. G. B. Hocker and W. K. Burns, *IEEE J. Quantum Electron.* **QE-11**, 270 (1975).
15. The Sellmeier expression used was $\Delta n_e^2 = a_1 + a_2/(\lambda^2 - a_3^2)$. The coefficients for the PE and APE waveguides are, respectively, $a_1 = 7.43 \times 10^{-3}$, $a_2 = 2.64 \times 10^{-3}$, $a_3 = 0.336$ and $a_1 = 3.43 \times 10^{-5}$, $a_2 = 1.10 \times 10^{-5}$, $a_3 = 0.326$.